

ORIGINAL RESEARCH PAPER

Photocatalytic Decolorization of Methylene Blue by N-doped TiO₂ Nanoparticles Prepared Under Different Synthesis Parameters

Shimelis Kebede Kassahun^{1,2,*}, Zebene Kiflie¹, Dong Woo Shin², Sam Sik Park²

¹School of Chemical and Bio Engineering, Addis Ababa Institute of Technology, Addis Ababa University, Addis Ababa, Ethiopia.

²Nano Co., Ltd. 60 Magong-gongdan-ro, Cheongni, Sangju, Gyeongbuk, South Korea.

Received: 2017-05-01

Accepted: 2017-06-20

Published: 2017-07-10

ABSTRACT

Although several studies concerning the preparation of nitrogen doped titanium dioxide visible-light active photocatalyst have already been reported, the effects of dopant concentration and calcination temperature have been rarely investigated. This paper focuses on the preparation of nitrogen doped titanium dioxide (N-doped TiO₂) under different calcination temperature and nitrogen dopant concentration synthesizes by sol-gel method. The physicochemical characteristics of the prepared samples were examined using X-ray photoelectron spectroscopy (XPS), X-ray diffractometer (XRD), Brunauer Emmett Teller (BET) analyzer, and UV-Vis spectrometer. Methylene blue was used in this study as a test chemical. The results demonstrated that the sample prepared under calcination temperature of 600 °C show 8.33 and 5.57 % of rutile TiO₂ phase depends on the dopant concentration. Furthermore, the sample prepared at a lower calcination temperature of 400 °C and nitrogen to titanium (N/Ti) molar ratio of 2 and 6 exhibited larger specific surface area of 80.18 and 77.07 m²g⁻¹, respectively. The photoactivity of the catalyst was also investigated on methylene blue decolorization using the different N-doped TiO₂ sample. The experiments demonstrated that the sample prepared at higher N/Ti molar ratio (6) and lower calcination temperature (400 °C) demonstrates about 80 % efficiency under visible light. It was concluded that the higher photoactivity of the N-doped sample prepared at higher dopant concentration and lower calcination temperature is due to synergistic effects of higher surface area, smaller crystal size and higher nitrogen content in the crystal lattice of TiO₂.

Keywords: Calcination Temperature, Dopant Concentration, Nitrogen-doped Titania, Sol-gel, Visible-light Active.

How to cite this article

Kassahun S K, Kiflie Z, Shin D W, Park S S. Photocatalytic Decolorization of Methylene Blue by N-doped TiO₂ Nanoparticles Prepared Under Different Synthesis Parameters. J. Water Environ. Nanotechnol., 2017; 2(3): 136-144. DOI: 10.22090/jwent.2017.03.001

INTRODUCTION

Recently, heterogeneous photocatalysis emerged as alternative technologies for environmental protection and cleaning. In this regard, semiconductor oxides such as titanium dioxide become the most popular choice because of its functionality and application [1]. Various applications of TiO₂ photocatalyst had

*Corresponding Author Email: shimelis.kebede@aait.edu.et; Tel.: +251 911557740; fax: +251 111239480.

been investigated that include degradation of organic pollutants [2], inactivation of pathogenic microorganisms from water and air [3], and degradation of dyes [4,5]. The basic mechanism of TiO₂ photocatalysis involves three major steps: (i) light absorption and generation of electron-hole pairs; (ii) separation of charge carriers; and (iii) oxidation and reduction reactions at the surface of semiconductor [6]. These leads to the

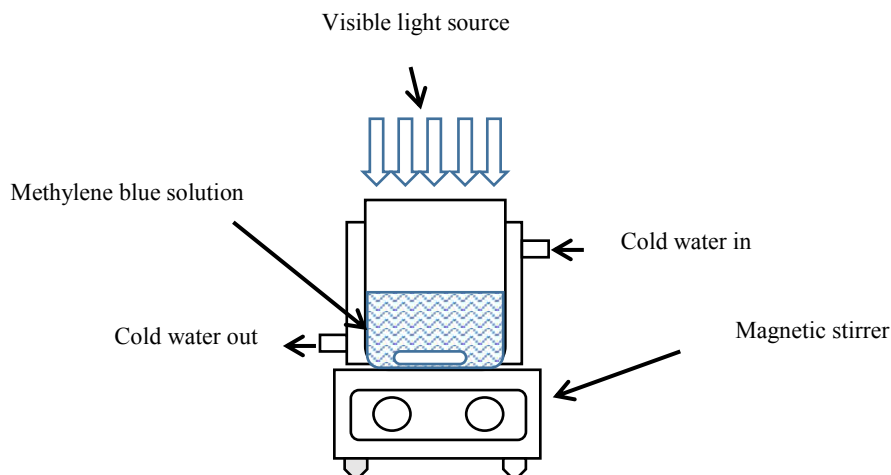


Fig. 1. Schematic diagram of slurry photoreactor.

formation of hydroxyl radical and superoxide radical anions which are the primary oxidizing species in the photocatalytic oxidation processes [7]. Non-toxicity, inexpensiveness, photochemical stability, and strong redox power in presence of oxygen and water are the unique characteristics of TiO₂ [8]. One of the major drawbacks of pure TiO₂ in practical application is its only activated by UV light which only accounts about 5 % of the solar radiation reaching the surface of the earth [9,10].

Chemical modification with doing, incorporation of foreign atoms in the titanium dioxide (TiO₂) crystal structure is one of the well-known strategies in order to synthesize visible-light active TiO₂ photocatalyst. Several researchers have pointed out non-metal doping is one of the best option to facilitate visible-light absorption as well as to improve recombination [11]. Among non-metals, nitrogen doping has been the most effective way for shifting the absorption edge of TiO₂ toward visible-light region through band gap reducing and improve the photoelectrochemical properties of the TiO₂ [12].

The development of visible-light-active TiO₂ nanoparticles using sol-gel method is highly dependent on several synthesis parameters. However, dopant concentration and calcination temperature have synergistic effects on the characteristics of the N-doped TiO₂. In the present work, we have synthesized N-doped TiO₂ photocatalysts using sol-gel methods and investigated the photoactivity at selected calcination temperature and dopant concentration. Furthermore, the effects of calcination temperature and dopant concentration on chemical and

physical properties were investigated using X-ray photoelectron spectroscopy (XPS), X-ray diffractometer (XRD), Brunauer-Emmett-Teller (BET) specific surface area, UV-vis spectroscopy (UV-vis).

EXPERIMENTAL

Catalyst Preparation

The preparation of nitrogen-doped titanium dioxide (N-doped TiO₂) was carried out by a sol-gel technique using ammonia solution (28 %) as a nitrogen source. The synthesis of N-doped TiO₂ was made using 20 mL of Titanium (IV) isopropoxide (TTIP) (98 %) as titanium precursor and 100 mL of ethanol (99.9 %) which were vigorously mixed together for 10 min in an ice bath. The solution was adjusted to pH =1 with nitric acid (60 %). Subsequently, different amounts of an aqueous solution of ammonia were adjusted to give N/Ti molar ratios of 2, and 6 were and stirred vigorously for 2 h. The obtained sol was aged for 24 h at room temperature to allow further hydrolysis and then dried in an oven dryer at 90 °C for 16 h. Finally, the resulting powder was ground and calcined at 400 and 600 °C for 4 h in a muffle furnace. The heating rate used was 5 °C min⁻¹. The N-doped TiO₂ samples were designated as

xNTyz, where x, y, and z, respectively, denote the N/Ti molar ratio, the calcination temperature, and time.

Catalyst Characterization

The atomic compositions of the doped and undoped TiO₂ samples were determined with X-ray photoelectron spectroscopy (XPS) (Thermo

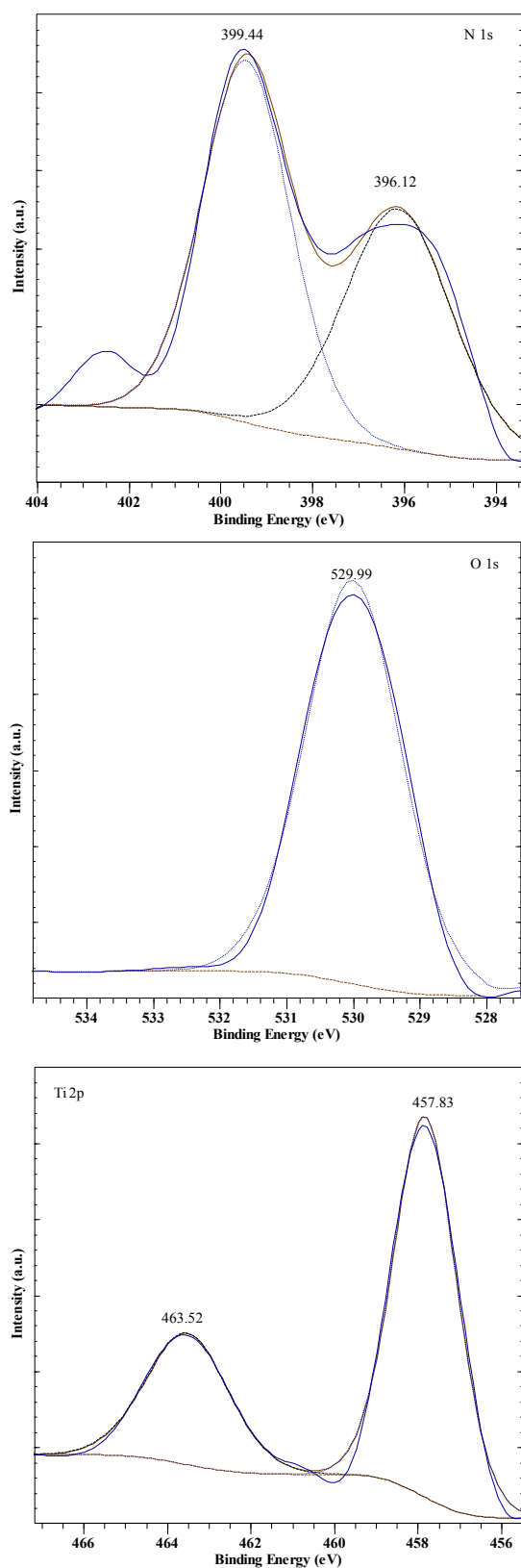


Fig. 2. Selected XPS spectra of N-doped TiO₂ sample (2NT64).

Scientific ESCALAB 250Xi). The binding energy of hydrocarbon (C 1s: 284.8 eV) was used as an internal standard for the correction of charging shift. The crystal structure of the N-doped sample was evaluated by X-ray diffractometer (XRD) using D8 advance with Cu-K α radiation ($\lambda=0.15406$), accelerating voltage and current (40 kV, 25 mA) at scan rate 0.017° per second in the range of $2\theta = 20^\circ$ to 85° . The average crystallite sizes of anatase and rutile phases were determined with the Scherrer equation. The weight fractions of the two phases were calculated using Spurr and Myers equation. Specific surface area of each sample was analyzed by Brunauer Emmett Teller (BET) method using Micromeritics, Tristar II 3020. UV/Vis/NIR Spectrophotometer (Hitachi, U-4100) was used to scan UV-vis spectra of the N-doped TiO₂ sample.

Photodecolorization of Methylene Blue

The photoactivity of N-doped TiO₂ nanoparticles was investigated using methylene blue (MB) as a model chemical in batch photoreactor under visible-light irradiation (Fig. 1). 250 ml jacketed glass reactor was used as photoreactor for all experiments in which visible-light was provided by Osram lamp (50 PARA30) with a wavelength of 400 –700 nm. During this process, 1.0 g L⁻¹ of the prepared powder was suspended in 100 ml of 10 ppm methylene blue solution (pH 7). The solution was continuously stirred with a magnetic stirrer 150 rpm to ensure homogenous mixing during 3 h irradiation period. Prior to proceeding to photoactivity test, the solution was stirred further for additional 30 minutes in dark environment to create adsorption-desorption equilibrium. After which, 10 ml of aliquots were taken from the reactor and filtered using 45 μ m syringe filter, the MB concentration of the supernatant was then analyzed with a portable spectrometer (DR 2700, Hach) at 664 nm wavelength absorbance.

The MB decolorization efficiency (R) was calculated using the following equation:

$$R(\%) = \frac{100(C_o - C_f)}{C_o} \quad (1)$$

Where C_o and C_f are the concentrations of methylene blue (mgL⁻¹) before and after visible-light irradiation. For control run, the methylene blue solution was exposed to visible light without the addition of catalyst for the same operational condition.

Table 1. Crystal size and phase composition for different N-doped TiO₂ sample.

Sample	Crystal phase composition (%)		Crystal size (nm)	
	Anatase	Rutile	Anatase	Rutile
2NT44	100	-	10.05	-
2NT64	91.67	8.33	22.78	55.08
6NT44	100	-	10.28	-
6NT64	94.43	5.57	23.84	58.26

RESULTS AND DISCUSSION

XPS Analysis

Selected XPS spectra N-doped sample prepared at N/Ti molar ratio of 2 and calcination temperature of 400 °C is shown in Fig. 1. For comparison, the atomic concentration of nitrogen atom and binding energies for N-doped TiO₂ samples are presented in Table 3. In all the samples two main peaks were detected, the first peaks at binding energies of around 400 eV and the second peaks are found at about 396 to 397. The exact positions of N atoms are still unclear and under debates. Many previously done studies assigned the position at the various locations from 395-404 eV binding energy based on their preparation routes and nitrogen source. However, in some of the well-known articles, the binding energy of N at 396 eV was surely assigned for atomic β-N [13–15]. This binding energy can be further extended to around 397 eV [16,17]. At this site, a substitutional replacement of oxygen by nitrogen takes place within TiO₂ crystal lattice in the form of Ti-N-Ti entity and may act, for visible-light, as the active site [18]. On the other hand, for interstitial N-doped TiO₂, such as Ti-N-O and/or Ti-O-N oxynitride, there is no common agreement. Generally, the peak approximate to 400 eV is assigned for interstitial N-doping [14,19]. Furthermore, the amount of nitrogen content was found significantly dependent on calcination temperature. In comparison, the sample prepared at higher calcination temperature shows the lower percentage of atomic concentration. This is due to a higher calcination temperature result in removal of nitrogen from the TiO₂.

XRD Analysis

Fig. 3 shows the XRD patterns of N-doped TiO₂ samples namely 6NT64, 6NT44, 2NT64 and 2NT44 prepared at N/Ti molar ratio of 6 and 2 and a calcination temperature of 400 °C and 600 °C. The XRD patterns of anatase and rutile phases are in good agreements with a reference (JCPDS) Card No 21-1272 and 21-1276 of TiO₂, respectively. As shown from the Fig. the typical anatase crystal

phase was appeared at the samples calcined at 400 °C. On the other hand, rutile phase of the TiO₂ appears at the different percentage for the sample synthesize at a calcination temperature of 600 °C. At the same calcination temperature of 600 °C, the percentage of rutile decreased from 8.33 % to 5.57 % when the N/Ti molar ratio increase from 2 to 6 (Table 1). This revealed that the anatase to rutile phase transformation or degree of crystallinity can be retarded at higher dopant concentration [20]. It has been reported that the addition of nitrogen dopant can improve the thermal stability of the TiO₂ catalyst [21]. Furthermore, the average crystal size significantly decreases when the temperature increases from 400 °C to 600 °C for both selected dopant concentration (N/Ti molar ratio of 2 and 6). This is due to the crystal can be aggregated and form a bigger crystal at higher calcination temperature [20]. It has been also indicated the crystallite size slightly increases as the N/Ti molar ratio increases from 2 to 6. It is known that the photocatalytic activity of the TiO₂ catalyst is highly dependent on crystal size and crystallinity [22,23].

Nitrogen Adsorption-desorption

To examine the effects of nitrogen dopant concentrations on the pore structure of samples, a set of nitrogen adsorption-desorption tests was carried out and their isotherms were presented in Fig. 4. According to IUPAC physisorption isotherms classification, the N-doped TiO₂ samples prepared at 400 °C showed a classification of type IV adsorption isotherms with narrow H2 hysteresis loop at around medium relative pressure. On the other hand, for calcination temperatures of 600 °C, the adsorption isotherm shifted to type V and H3 hysteresis loop at higher relative pressure. The two hysteresis loops at lower and higher relative pressure are raised from smaller and larger mesopore characteristics, respectively. A plausible explanation can be at higher calcination temperature there is an expansion of mesopores and consequently the formation of bigger pores [24]. Furthermore, Specific surface area, pore

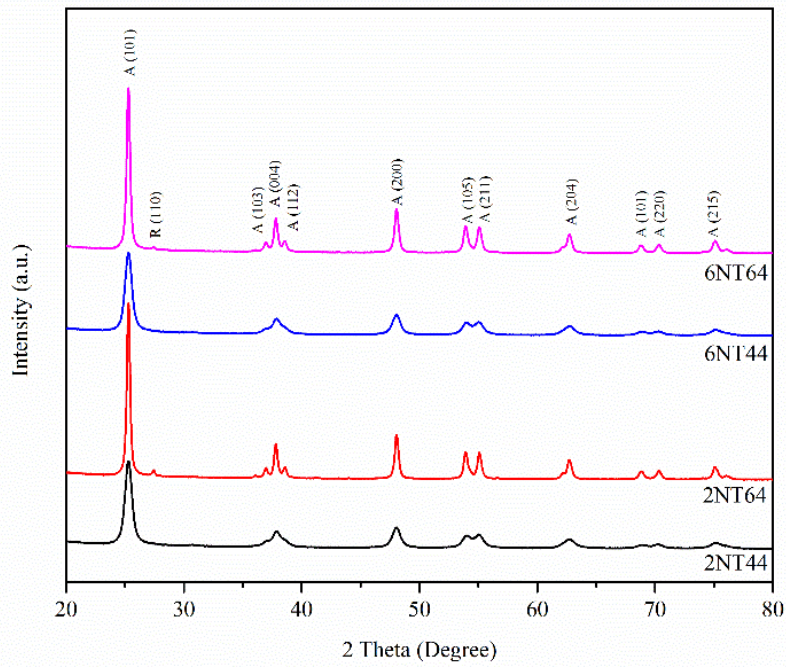


Fig. 3. XRD patterns for different N-doped TiO₂ sample.

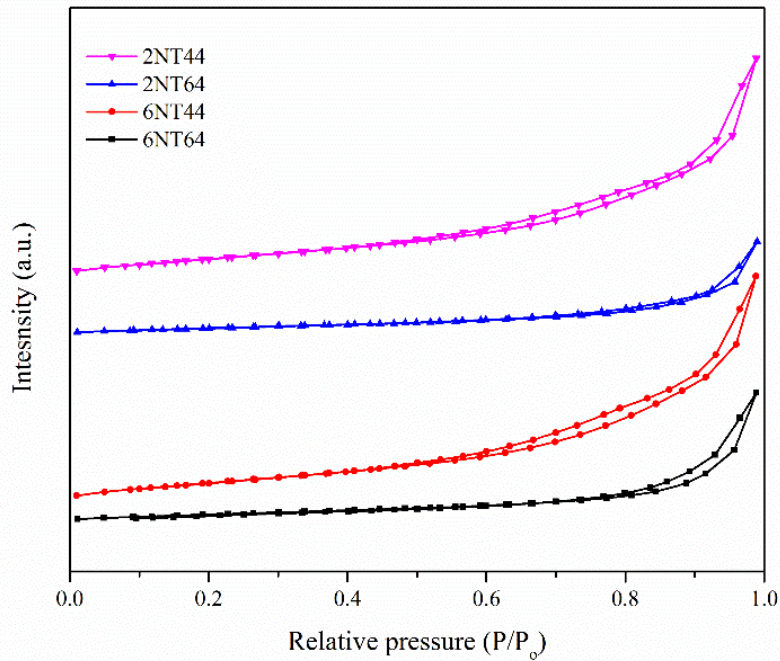


Fig. 4. Adsorption-desorption isotherm for different N-doped TiO₂ sample.

Table 2. BET surface area, total pore volume and average pore diameter for different N-doped TiO₂ sample.

Sample	BET surface area (m ² g ⁻¹)	Total pore volume (m ³ g ⁻¹)	Average pore diameter (nm)
2NT44	80.18	0.23	11.69
2NT64	30.81	0.13	16.87
6NT44	77.07	0.23	11.60
6NT64	27.97	0.10	13.56

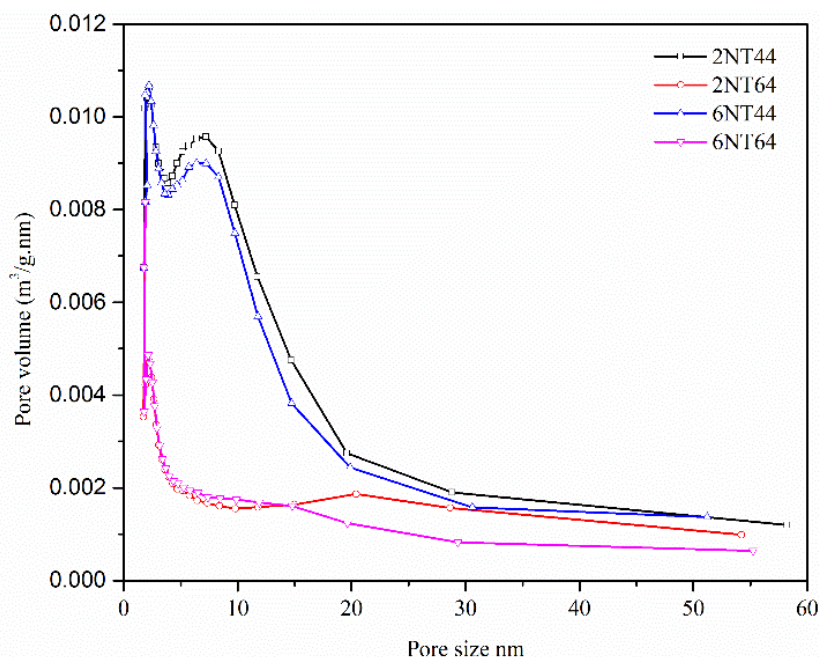


Fig. 5. Pore size distribution for different N-doped TiO₂ sample.

volume, and pore size were evaluated according to BET and BJH methods and the data shown in Fig. 5 and Table 1. The specific surface areas and corresponding total pore volume were indicated a decreasing trend (for both N/Ti molar ratio of 2 and 6) with an increase in calcination temperature from 400 °C to 600 °C. Decreased specific surface area is due to catalyst aggregation at the higher temperature [25].

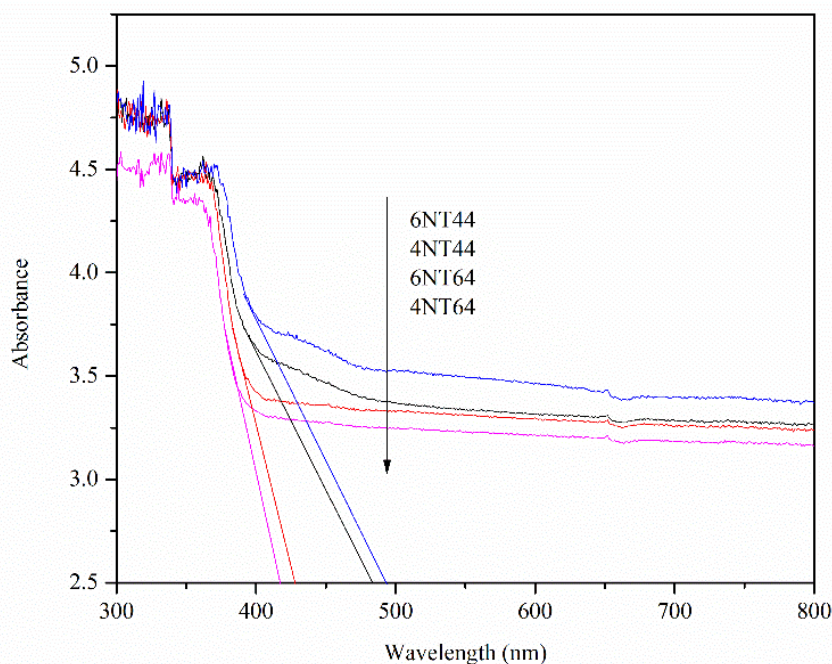
Optical Analysis

The UV-vis spectra for the N-doped TiO₂ sample prepared at different condition were presented in Fig. 6. The absorption edges of each sample were shifted to the visible-light spectra region corresponding to the dopant concentration. The optical absorption intensity in the wavelength found to be 420, 430, 480 and 495 nm for the sample namely 6NT44, 4NT44, 6NT64, and 4NT64, respectively. Many researchers pointed out that the preparation of N-doped TiO₂ shows spectra shift toward the visible-light region [26]. Asahi et al. claim that its visible-light photoactivity can be related to narrowed band gap by mixing of nitrogen 2p and oxygen 2p state in the valence band caused by substitutional doping [13]. In contrast, Burda and his coworker have stated that the extra electronic states just above the valence band edge were the main reasons behind this phenomenon [19].

Investigation of Photoactivity

To investigate the photoactivity of the N-doped TiO₂ sample, MB photo decolorization tests were carried out and the data presented in Fig. 7. As demonstrated in the Fig., the sample prepared at lower calcination temperature (400 °C) and higher N/Ti molar ratio (6) exhibited improved photocatalytic activities. As a matter of facts, the highest photoactivity shown by the conditions can be due to the synergistic effects of higher surface area, lower crystal size and higher nitrogen content [20,27–30]. Whereas, the two samples prepared at higher calcination temperature (600 °C) for N/Ti molar ratio of 2 and 6 shows the list activity.

Nosaka et al [31], have studied the photocatalytic performance nitrogen doped TiO₂ prepared from commercially available TiO₂ powders and an organic compound such as urea and guanidine as a nitrogen source. According to their findings, the prepared N-doped TiO₂ powders exhibited photocatalytic activity for the decomposition of 2-propanol in aqueous solution under visible- light irradiation. Furthermore, they have observed that the visible photocatalytic activity was decreased with the higher calcination temperature (550 °C). Qin et al. [32]. have also investigated the effects of dopant concentration on photocatalytic properties of N-doped TiO₂. The photocatalytic activities

Fig. 6. UV-Vis spectra for different N-doped TiO₂ sample.Table 3. Percentage atomic concentration and binding energies of nitrogen for different N-doped TiO₂ sample.

Sample	N 1s (% at. Conc)	Binding Energies (eV)	
2NT44	1.03	399.87	396.04
2NT64	0.45	399.44	396.12
6NT44	2.08	400.01	397.07
6NT64	0.53	400.54	396.63

were estimated in the system of methyl orange aqueous solution (MO) under UV and visible light, respectively. The photodegradation of 2-mercaptobenzothiazole aqueous solution (MBT) under visible-light was also included in their study. They have pointed out N/Ti proportion of 4mol % exhibited the highest visible-light activity.

CONCLUSION

A visible-light active N-doped TiO₂ catalysts have been synthesized by sol-gel methods at different calcination temperature and dopant concentration. All N-doped TiO₂ samples show a mesoporous structure and the sample prepared at lower calcination and higher dopant concentration results higher specific surface area. The anatase to rutile phase transformation was also retarded at higher nitrogen dopant concentration. Furthermore, the amount of nitrogen doped in TiO₂ crystal was found significantly dependent

on calcination temperature. The 6NT44 sample showed higher photocatalytic activity (about 80 %) in decolorization of methylene blue in aqueous solution under visible-light irradiation.

ACKNOWLEDGEMENTS

The authors would like to acknowledge the support from Addis Ababa University, Addis Ababa Institute of Technology, National Institute for International Education (NIIED), Korean Ministry of Education scholarship program (# KGSP-GRA-2015-170) and Gyeongsang National University. We would like also to extend our appreciation for Nano Co., Ltd for allowing us to use its advanced research facilities.

CONFLICT OF INTEREST

The authors declare that there are no conflicts of interest regarding the publication of this manuscript.

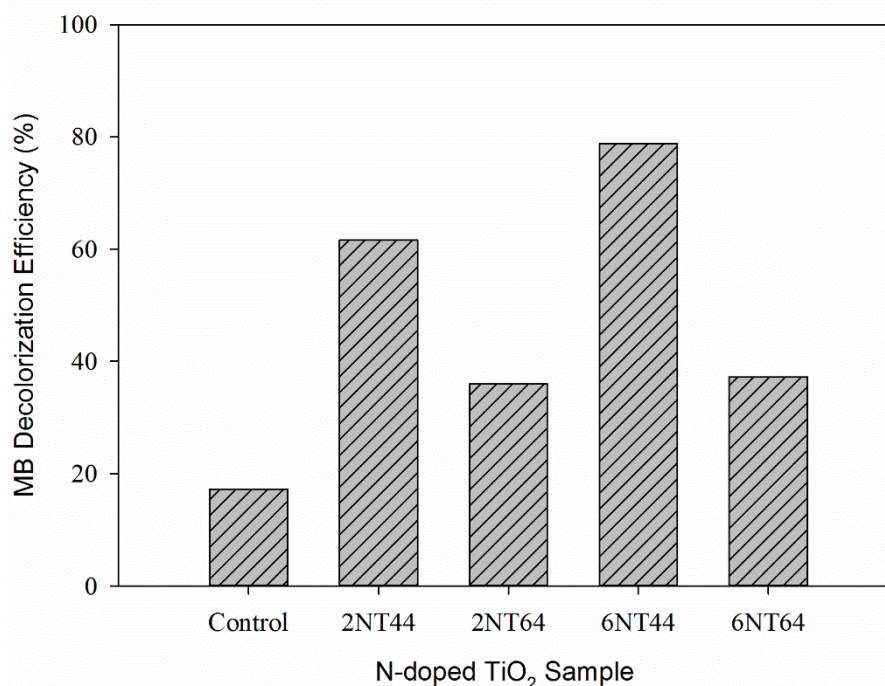


Fig. 7. Photodecolorization of methylene blue under visible light irradiation.

REFERENCE

- Zhihua X, Jiaguo Y. A novel solid-state electrochemiluminescence sensor based on Ru(bpy)₃²⁺ + immobilization on TiO₂ nanotube arrays and its application for detection of amines in water. *Nanotechnology*. 2010;21(24):245501.
- Huang X-h, HU C. Preparation and characterization of visible-light-active nitrogen-doped TiO₂ photocatalyst. *Journal of Environmental Sciences*. 2005;17(4):562-5.
- Ferrari-Lima AM, Marques RG, Gimenes ML, Fernandes-Machado NRC. Synthesis, characterisation and photocatalytic activity of N-doped TiO₂-Nb₂O₅ mixed oxides. *Catalysis Today*. 2015;254:119-28.
- Khataee AR, Zarei M, Moradkhannejhad L, Nourie S, Vahid B. Nitrogen Doping of Commercial TiO₂ Nanoparticles for Enhanced Photocatalytic Degradation of Dye Under Visible Light: Central Composite Design Approach. *Advanced Chemistry Letters*. 2013;1(1):24-31.
- Natarajan K, Natarajan TS, Bajaj HC, Tayade RJ. Photocatalytic reactor based on UV-LED/TiO₂ coated quartz tube for degradation of dyes. *Chemical Engineering Journal*. 2011;178:40-9.
- Zaleska A. Doped-TiO₂: A Review. *Recent Patents on Engineering*. 2008;2(3):157-64.
- Wu MJ, Bak T, O'Doherty PJ, Moffitt MC, Nowotny J, Bailey TD, et al. Photocatalysis of titanium dioxide for water disinfection: challenges and future perspectives. *International Journal of Photochemistry*. 2014;2014.
- Cani D, Pescarmona PP. Macroscopic TiO₂-SiO₂ porous beads: Efficient photocatalysts with enhanced reusability for the degradation of pollutants. *Journal of Catalysis*. 2014;311:404-11.
- Tang W, Qiu K, Zhang P, Yuan X. Synthesis and photocatalytic activity of ytterbium-doped titania/diatomite composite photocatalysts. *Applied Surface Science*. 2016;362:545-50.
- Caratto V, Setti L, Campodonico S, Carnasciali MM, Botter R, Ferretti M. Synthesis and characterization of nitrogen-doped TiO₂ nanoparticles prepared by sol-gel method. *Journal of Sol-Gel Science and Technology*. 2012;63(1):16-22.
- Pelaez M, Nolan NT, Pillai SC, Seery MK, Falaras P, Kontos AG, et al. A review on the visible light active titanium dioxide photocatalysts for environmental applications. *Applied Catalysis B: Environmental*. 2012;125:331-49.
- Khan M, Cao W. Development of photocatalyst by combined nitrogen and yttrium doping. *Materials Research Bulletin*. 2014;49:21-7.
- Asahi R, Morikawa T, Ohwaki T, Aoki K, Taga Y. Visible-Light Photocatalysis in Nitrogen-Doped Titanium Oxides. *Science*. 2001;293(5528):269-71.
- Sato S, Nakamura R, Abe S. Visible-light sensitization of TiO₂ photocatalysts by wet-method N doping. *Applied Catalysis A: General*. 2005;284(1):131-7.
- Saha NC, Tompkins HG. Titanium nitride oxidation chemistry: An x-ray photoelectron spectroscopy study. *Journal of Applied Physics*. 1992;72(7):3072-9.
- Buzby S, Barakat MA, Lin H, Ni C, Rykov SA, Chen JG, et al. Visible light photocatalysis with nitrogen-doped titanium dioxide nanoparticles prepared by plasma assisted chemical vapor deposition. *Journal of Vacuum Science & Technology B: Microelectronics and Nanometer Structures Processing, Measurement, and Phenomena*. 2006;24(3):1210-4.
- Chen X, Burda C. The Electronic Origin of the Visible-

- Light Absorption Properties of C-, N- and S-Doped TiO₂ Nanomaterials. *Journal of the American Chemical Society*. 2008;130(15):5018-9.
18. Mollavali M, Falamaki C, Rohani S. Preparation of multiple-doped TiO₂ nanotube arrays with nitrogen, carbon and nickel with enhanced visible light photoelectrochemical activity via single-step anodization. *International Journal of Hydrogen Energy*. 2015;40(36):12239-52.
 19. Wang J, Tafen DN, Lewis JP, Hong Z, Manivannan A, Zhi M, et al. Origin of Photocatalytic Activity of Nitrogen-Doped TiO₂ Nanobelts. *Journal of the American Chemical Society*. 2009;131(34):12290-7.
 20. Lin Y-H, Weng C-H, Srivastav AL, Lin Y-T, Tzeng J-H. Facile synthesis and characterization of N-doped TiO₂ photocatalyst and its visible-light activity for photo-oxidation of ethylene. *J Nanomaterials*. 2015;2015:1-10.
 21. Samsudin EM, Abd Hamid SB, Juan JC, Basirun WJ, Kandjani AE, Bhargava SK. Controlled nitrogen insertion in titanium dioxide for optimal photocatalytic degradation of atrazine. *RSC Advances*. 2015;5(55):44041-52.
 22. Kongsong P, Sikong L, Niyomwas S, Rachpech V. Photocatalytic Degradation of Glyphosate in Water by N-Doped SnO₂/TiO₂ Thin-Film-Coated Glass Fibers. *Photochemistry and Photobiology*. 2014;90(6):1243-50.
 23. Kongsong P, Sikong L, Niyomwas S, Rachpech V. Photocatalytic Antibacterial Performance of Glass Fibers Thin Film Coated with N-Doped SnO₂/TiO₂. *The Scientific World Journal*. 2014;2014:9.
 24. Zhu J, Wang T, Xu X, Xiao P, Li J. Pt nanoparticles supported on SBA-15: Synthesis, characterization and applications in heterogeneous catalysis. *Applied Catalysis B: Environmental*. 2013;130:197-217.
 25. Yu H, Zheng X, Yin Z, Tag F, Fang B, Hou K. Preparation of Nitrogen-doped TiO₂ Nanoparticle Catalyst and Its Catalytic Activity under Visible Light* *Supported by the Science and Technology Research Program of Chongqing Education Commission (KJ050702), and the Natural Science Foundation Project of Chongqing Science and Technology Commission (No.2007BB7208). *Chinese Journal of Chemical Engineering*. 2007;15(6):802-7.
 26. Lee HU, Lee SC, Choi S, Son B, Lee SM, Kim HJ, et al. Efficient visible-light induced photocatalysis on nanoporous nitrogen-doped titanium dioxide catalysts. *Chemical Engineering Journal*. 2013;228:756-64.
 27. Lei XF, Xue XX, Yang H, Chen C, Li X, Niu MC, et al. Effect of calcination temperature on the structure and visible-light photocatalytic activities of (N, S and C) co-doped TiO₂ nano-materials. *Applied Surface Science*. 2015;332:172-80.
 28. Lin Y-T, Weng C-H, Hsu H-J, Lin Y-H, Shiesh C-C. The Synergistic Effect of Nitrogen Dopant and Calcination Temperature on the Visible-Light-Induced Photoactivity of N-Doped TiO₂. *International Journal of Photoenergy*. 2013;2013:13.
 29. Nolan NT, Synnott DW, Seery MK, Hinder SJ, Van Wassenhoven A, Pillai SC. Effect of N-doping on the photocatalytic activity of sol-gel TiO₂. *Journal of Hazardous Materials*. 2012;211:88-94.
 30. Wu X, Fang S, Zheng Y, Sun J, Lv K. Thiourea-Modified TiO₂ Nanorods with Enhanced Photocatalytic Activity. *Molecules*. 2016;21(2).
 31. Yoshio N, Masami M, Junichi N, Atsuko YN. Nitrogen-doped titanium dioxide photocatalysts for visible response prepared by using organic compounds. *Science and Technology of Advanced Materials*. 2005;6(2):143.
 32. Qin H-L, Gu G-B, Liu S. Preparation of nitrogen-doped titania using sol-gel technique and its photocatalytic activity. *Materials Chemistry and Physics*. 2008;112(2):346-52.